

表面制御透過実験装置の製作と性能試験

波多野 雄治、能村 衛、渡辺 国昭
富山大学水素同位体科学研究センター
〒930-8555 富山市五福 3190

Alexander I. Livshits, Andrei O. Busnyuk
Bonch-Bruyevich University of Telecommunications
61 Moika, St. Petersburg 191186, Russia

中村 幸男、大藪 修義
核融合科学研究所
〒509-5292 岐阜県土岐市下石町 322-6

Construction and Performance Test of Apparatus for Permeation Experiments with Controlled Surfaces

Yuji Hatano, Mamoru Nomura and Kuniaki Watanabe
Hydrogen Isotope Research Center, Toyama University
Gofuku 3190, Toyama 930-8555, Japan

Alexander I. Livshits, Andrei O. Busnyuk
Bonch-Bruyevich University of Telecommunications
61 Moika, St. Petersburg 191186, Russia

Yukio Nakamura, Nobuyoshi Ohyabu
National Institute for Fusion Science
Oroshi-cho, Toki 509-5292, Japan

(Received March 30, 2002; Accepted December 20, 2002)

Abstract

A new apparatus was constructed to examine gas-, atom- and plasma-driven permeation of hydrogen isotopes through group VA metal membranes with precisely controlled surface states. Absorption and desorption experiments are also possible. The new apparatus consists of two vacuum chambers, an upstream chamber and a downstream chamber, separated by a specimen membrane. Both chambers are evacuated by turbo-molecular pumps and sputter-ion pumps. The upstream chamber is equipped with Ta filaments serving as atomizers in atom-driven permeation experiments and cathodes in plasma-driven permeation experiments. The specimen membrane is formed into a tubular shape and electrically isolated from the chamber. Hence, ohmic heating of

the membrane is possible, and this feature of the membrane is suitable for surface cleaning by high-temperature heating and impurity doping for the control of surface chemical composition through surface segregation. Both chambers were evacuated to 1×10^{-7} Pa after baking. The main component of residual gas was H_2 , and the partial pressures of impurity gases other than H_2 were ca. 1×10^{-8} Pa. Gas- and atom-driven permeation experiments were successfully carried out with hydrogen gas for Nb membrane activated by heating in vacuum at 1173 K. Superpermeation was observed in the atom-driven permeation experiments. Absorption experiments with a clean surface were also carried out. The surface was, however, cleaned only partially, because the temperature distribution was not uniform during high-temperature heating. Nevertheless, surface cleanliness was retained during absorption experiments under the present vacuum conditions. A new membrane assembly that will enable a uniform temperature distribution is now under construction.

1. Introduction

Surfaces of metals are usually covered by thin layers of non-metallic impurities such as oxygen and carbon. Hence, the investigation on interaction between hydrogen isotopes and metal surfaces covered by impurity layers are important in various fields of science and technology such as surface physics and chemistry, catalysis, hydrogen energy and nuclear fusion systems. The precise control of surface chemical composition, however, is required to carry out the systematic study. This kind of study is carried out in ultra-high vacuum (UHV) apparatuses in most cases, but the control of surface composition is generally difficult even in UHV. This is because dissolution of impurities into metal bulk can take place as well as evaporation from surface to gas phase.

Recently, the present authors have found out that the recombination rate constant of deuterium at Nb surface systematically decreases with increasing oxygen content in the bulk because of the surface segregation of oxygen [1]. The control of surface composition by surface segregation is promising technique, because impurity coverage is determined thermodynamically by the impurity concentration in the bulk and the heat of segregation.

On the other hand, metals covered by thin impurity layers have enormous capabilities for permeation and absorption for suprathreshold atoms and ions of hydrogen isotopes [2,3]. Hence, metallic membranes and panels covered by such impurity layers can be applied for particle control and separation of D/T from He in fusion devices [3-9]. Such high capabilities for permeation and absorption are due to the suppression of reemission of hydrogen isotopes from incident surfaces by non-metallic impurities. Reduction in the impurity coverage by sputtering degrades the absorption and permeation capabilities, and hence compensation for removed impurities is necessary to maintain the performance of membranes and panels under sputtering. Surface segregation of impurities from the bulk is promising also for the compensation of sputtered impurities.

The group VA metals (V, Nb and Ta) are candidates of pumping membrane and panel materials in fusion energy systems [5-9], hydrogen storage materials [10, 11] and membrane materials for hydrogen purification in hydrogen energy systems [12-14]. Hence, the present authors have started the systematic study on the interaction between the hydrogen isotopes and the surfaces of group VA metals covered by non-metallic impurities such as oxygen and sulfur by surface segregating technique. The main apparatuses used for this study are a surface analysis system (X-ray and ultraviolet photoelectron spectroscopy) and a permeation apparatus constructed recently. This permeation apparatus has capability to carry out gas-, atom- and plasma-driven permeation experiments with well-controlled surface chemical compositions as well as absorption/desorption experiments. One of the interesting features of the apparatus is the shape of specimen membrane; the membrane is in tubular form and not in sheet form as usual permeation apparatuses. This shape of membrane is beneficial for surface treatment. The present paper describes the characteristics of the permeation apparatus in detail as well as the results of performance tests.

2. Characteristics of permeation apparatus

A schematic description of the constructed permeation apparatus is shown in Fig. 1. This

apparatus consists of two UHV chambers, an upstream chamber and a downstream chamber, separated by a tubular specimen membrane. The upstream chamber comprises the main discharge chamber and auxiliary chamber, and analysis instruments such as pressure gauges are installed in the latter. Both upstream and downstream chambers were evacuated by turbo-molecular pumps (TMPs) and sputter-ion pumps (IPs). The conductance to the upstream IP can be adjusted to 0.1, 20 and 7000 L·s⁻¹ by moving diaphragms connected to the linear motion feedthrough. The total pressure is measured by Pirani gauges at high pressure region (0.13-1.3×10⁵ Pa) and ionization gauges at low pressure region (10⁻⁸-1.0 Pa). The partial pressure of each gas species are measured by quadrupole mass analyzers (QMAs). These pressure gauges and mass analyzers were calibrated with diaphragm gauges whose full scales are 1.33×10⁵ and 13.3 Pa. The maximum baking temperature is 673 K for the main discharge chamber and 473 K for the auxiliary and downstream

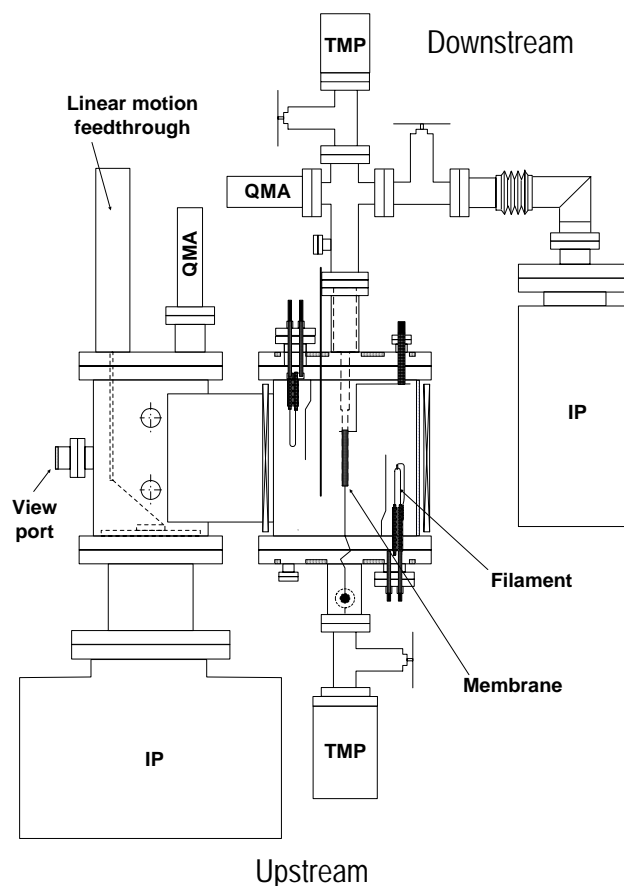


Fig. 1 Schematic description of constructed permeation apparatus.

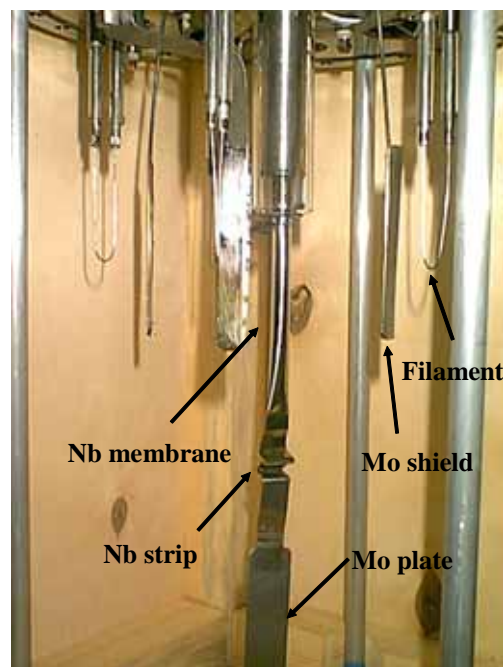


Fig. 2 Photo of upper flange of main discharge chamber.

chambers. Hydrogen, deuterium and other gases for surface modification such as O_2 are introduced into both chambers through variable-leak valves.

Figure 2 shows the upper flange of the main discharge chamber. This chamber is equipped with the specimen membrane and 9 Ta filaments whose diameter is 0.8 mm; 4 filaments are mounted on the upper flange and 5 filaments on the lower flange. Molybdenum shields are installed between the filaments and the specimen membrane to avoid the deposition of Ta on to the membrane. The filaments are used for two purposes: dissociation of hydrogen and deuterium molecules for atom-driven permeation experiments and electron emission for plasma-driven permeation experiments. In the latter case, the discharge is carried out by applying voltage (<120 V) between the filaments serving as cathode and the chamber wall serving as anode. The kinetic energy of incident ions onto the membrane was controlled by the bias voltage between the chamber wall and the specimen membrane. Magnets made of SmCo alloy are mounted on the outside of the chamber wall as shown in Fig. 3 to provide the multicusp magnetic field (see Fig. 4); the magnetic flux density in the chamber is ca. 0.01 T. The chamber wall is cooled by water during operation to avoid the increase in background pressure.

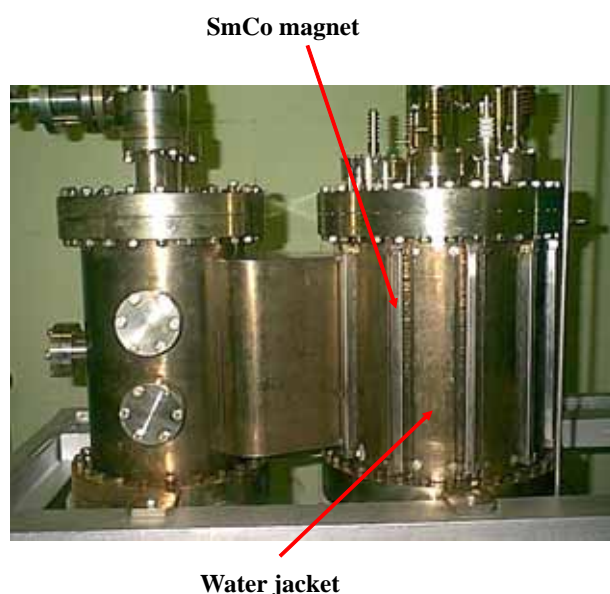


Fig. 3 Photo of main discharge chamber (right) and auxiliary chamber (left).

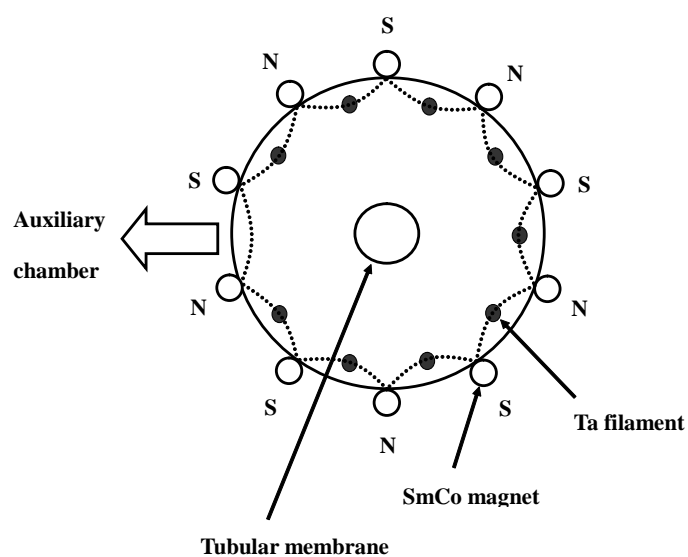


Fig. 4 Schematic description of multicusp magnetic field.

The details of Nb membrane assembly are shown in Fig. 5 as an example. The specimen membrane is formed into a tubular shape by laser welding in Ar atmosphere and electrically isolated from the chamber. This feature of membrane allows ohmic heating. One-end of the tubular membrane is closed by welding and connected to an electric feedthrough through Nb strip and Mo plate. The electric resistance of the Nb strip is the same as the membrane. The other end is kept open and connected hermetically to the downstream chamber through a stainless steel joint tube, larger stainless steel tube and ceramic insulation tube. Strips of Nb and Ni are connected to the upper part of membrane and the larger stainless steel tube as shown in this figure as electric leads. The stainless steel joint tube is heated ohmically to minimize the temperature gradient in the membrane near the connection part, and the temperature of joint tube is measured by W-Re thermocouple. The temperature of the membrane is measured also by W-Re thermocouple inserted in the membrane from the downstream side (not shown in the figure). Typical thickness of the membrane is 0.1 mm.

The capability for ohmic heating is very important feature for surface treatment. It has been reported that clean surfaces of Nb and Ta are available by heating in UHV up to 2300 K [15, 16]. The membrane can be easily heated up to this temperature at current around 240 A. In addition, only the temperature of the membrane is elevated except the Nb strip beneath the membrane, and hence gases for surface modification reacts only

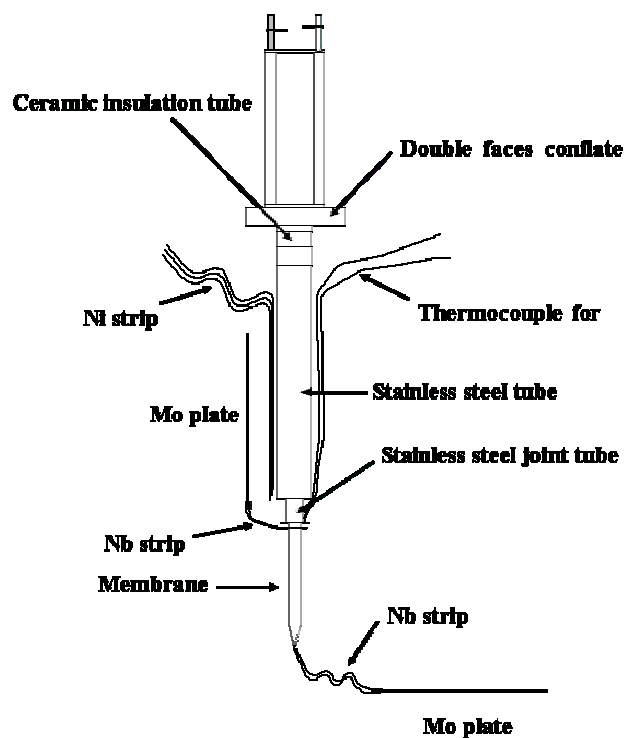


Fig. 5 Details of membrane assembly.

with Nb membrane and strip. Therefore, the amount of doped impurity can be estimated accurately. The high temperature heating (above 2000 K) for surface cleaning is carried out by an alternating current power supply and high capacity transformer (6.5 kW). A direct current power supply is used for temperature control during permeation and absorption/desorption experiments.

The expected flux of atoms and ions to the membrane during discharge are 10^{17} atoms·cm⁻²·s⁻¹ and 10^{15} ions·cm⁻²·s⁻¹, respectively. The flux of atoms by thermal dissociation is expected to be 10^{16} atoms·cm⁻²·s⁻¹.

3. Results of performance tests

3.1. Vacuum conditions

The residual pressure after baking at the maximum temperatures was 1×10^{-7} Pa in both upstream and downstream chambers. The mass spectrum of residual gas in the downstream chamber is shown in Fig. 6. The main residual gas was H₂, and small peaks of CO and H₂O were observed; the peak height of CO and H₂O was ca. 1/5 and 1/10 of that of H₂, respectively. It is plausible that the source of CO is the filament of QMA, and water vapor is the dominant residual gas other than H₂ when QMA is switched off. No significant difference was observed in the mass spectrum of residual gas in the upstream chamber.

The partial pressures of impurities such as H₂O, N₂ and O₂ were comparable to the background after introducing hydrogen to pressures below 1×10^{-3} Pa without any purification system. Above 1×10^{-3} Pa, those impurity gases were detected, and their partial

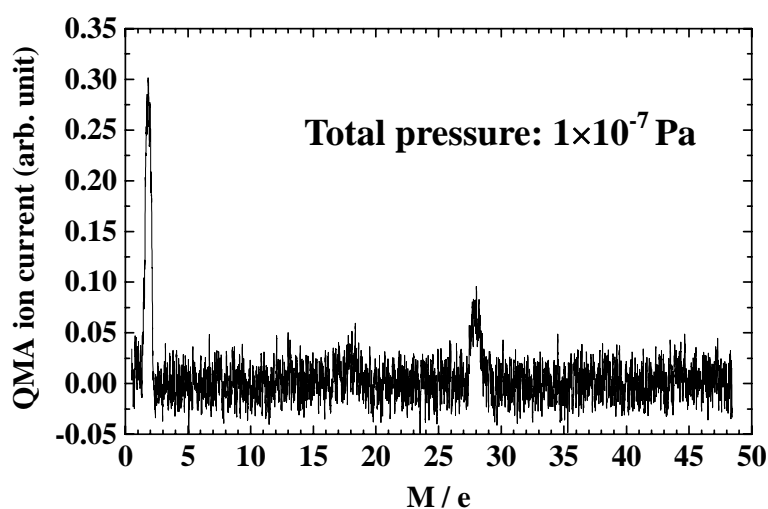


Fig. 6 Typical example of mass spectrum of residual gas in downstream chamber.

pressures increased to ca. 3×10^{-7} Pa after introducing hydrogen to 10^{-2} Pa. A hydrogen purification system is now under development for reduction in the partial pressures of impurities at high pressure operations.

3.2. Gas- and atom-driven permeation after activation of membrane at 1173 K

A niobium membrane was used for the performance test. The specimen membrane was activated by heating in vacuum up to 1173 K, and gas-driven permeation experiments were carried out with H_2 at 0.02 Pa of the upstream pressure. Figure 7 shows the steady state permeation probability χ of H_2 molecules striking the upstream surface together with corresponding downstream pressure. The permeation probability χ increases with temperature, and the activation energy of permeation E_P was estimated to be $42 \text{ kJ}\cdot\text{mol}^{-1}$. This value of E_P indicates that permeation rate is controlled by surface processes, i.e. sticking and recombination processes, and not by the diffusion process in the bulk. This is because E_P should take a negative value, $-22 \text{ kJ}\cdot\text{mol}^{-1}$, in the diffusion-limited case. Namely, E_P is determined by the activation energy of diffusion E_D and the heat of solution E_S as $E_P = E_D + E_S$ provided that the permeation rate is controlled by the bulk diffusion process, where $E_D = 10 \text{ kJ}\cdot\text{mol}^{-1}$ [17] and $E_S = -34 \text{ kJ}\cdot\text{mol}^{-1}$ [18] for Nb-H system.

The sticking coefficient of H_2 molecules α_m can be easily estimated from the permeation probability shown in Fig. 7. In the steady state, the flux of hydrogen penetrating into the membrane is equal to the sum of release flux from upstream and downstream surfaces:

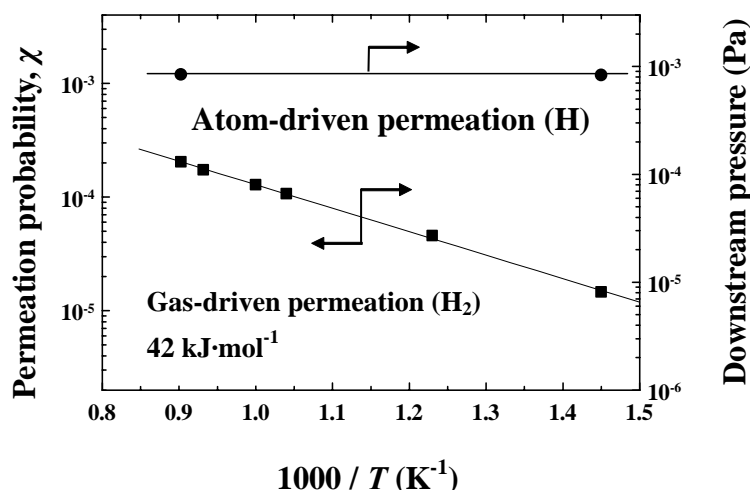


Fig. 7 Results of gas- and atom-driven permeation experiments after activation of Nb membrane at 1173 K.

$$\alpha_m \varphi_m = kr_u C_u^2 + kr_d C_d^2, \quad (1)$$

where φ_m is the flux of H₂ molecules striking the upstream surface, kr the recombination rate constant, C the hydrogen concentration in subsurface layer, and u and d indicate upstream and downstream sides, respectively. The permeation flux φ_P can be expressed as $\varphi_P = kr_d C_d^2$. The concentration gradient of hydrogen in the bulk is negligibly small in the surface-limited regime, and hence φ_P can be rewritten as

$$\varphi_P = \alpha_m \varphi_m \cdot kr_d / (kr_u + kr_d). \quad (2)$$

By assuming that kr on upstream and downstream surfaces are equal to each other ($kr_u = kr_d$), φ_P can be derived as $\varphi_P = \alpha_m \varphi_m / 2$. The permeation probability χ is expressed as $\chi = \varphi_P / \varphi_m = \alpha_m / 2$. The values of α_m thus obtained ranged from 2.7×10^{-5} (690 K) to 2.6×10^{-4} (1000 K). The sticking probability α_m takes a value around 0.1 provided that the surface of Nb membrane is clean [1, 16]. The values obtained are significantly smaller than that for clean surface, indicating that the surface is contaminated by impurity. This impurity appeared to come from metal bulk and not from gas phase. This is because the values of α_m obtained at various H₂ pressures were comparable to each other, while the partial pressures of impurities in the gas phase were dependent on H₂ pressure as described in 3.1. In the previous paper [1], the present authors found that oxygen segregates to the surface of Nb by vacuum heating. Hence, it is plausible that oxygen is the dominant surface impurity.

The sticking probability α_m is generally expressed as $\alpha_m = \alpha_{m0} \exp(-E_C / RT)$ where α_{m0} is the pre-exponential factor, E_C the potential barrier against dissociative chemisorption, R the gas constant and T temperature. The potential barrier E_C is negligibly small for the clean surfaces of transition metals and putted up by surface impurities [19]. It is widely accepted that both α_{m0} and E_C are independent of temperature, and the temperature dependence of α_m is determined only by this “constant” E_C . This idea is not correct when the impurity coverage at the surface is dependent on temperature through segregation/dissolution of impurities from/into the bulk. One of the main objectives of the present research project is to develop the phenomenological model to describe α_m

and kr by taking account of such temperature dependence of impurity coverage.

The atom-driven permeation experiments were also carried out by thermal atomization by Ta filaments and the results are shown in Fig. 7. In this case, only the downstream pressures during permeation experiments are indicated, because flux of atoms has not been measured and permeation probability of atoms could not be estimated. It is, however, clear that the downstream pressure increased by atomization. In addition, no temperature dependence was observed in the permeation rate in the case of atom-driven permeation, whereas the permeation rate increased with temperature in the case of gas-driven permeation as mentioned above. These observations correspond to the phenomenon called superpermeation. The mechanism of superpermeation can be explained as follows. In the case of atom-driven permeation, Eq. (2) can be rewritten as

$$\varphi_P = (1/2) \alpha_a \varphi_a \cdot kr_d / (kr_u + kr_d), \quad (3)$$

where α_a and φ_a are the sticking coefficient and the flux of hydrogen atom, respectively. Factor 1/2 is necessary to adjust the mass balance between atomic incidence and molecular release. In this case, φ_P can be expressed as $\varphi_P = \alpha_a \varphi_a / 4$ at $kr_u = kr_d$. The internal energy of hydrogen atom is higher than that of molecule by 2.24 eV, and hence atoms easily overcome E_C . Namely, α_a is close to unity and independent of temperature even at the surfaces covered by impurities [2,3,19]. Therefore, larger and temperature independent permeation (superpermeation) takes place under atomization.

3.3. Measurement of α_m after surface cleaning at high temperature

The membrane was heated gradually up to a high temperature (2323 K) and kept at this temperature for 15 s. During temperature elevation, significant release of CO was observed. It is plausible that oxygen and carbon present in the bulk as impurities were released mainly as CO.

After the high temperature heat treatment, the sticking coefficient of hydrogen molecules α_m was obtained by two different methods. In low temperature region where $T < 673$ K, α_m was estimated from the absorption rate of H_2 by the membrane measured by the following procedure.

First, pumping of the chambers was stopped overnight, and the membrane surfaces were deactivated by the exposure to residual gas of rather high pressure (10^{-4} Pa) at room temperature. The chambers were evacuated to UHV again, and H_2 gas was introduced into the upstream chamber to 1×10^{-5} Pa. After the establishment of very stable gas flow, the hydrogen introduction was stopped by pumping the backside of the variable-leak valve (VLV), in which the opening of VLV was kept constant. Then, the membrane was activated by heating at 1273 K for 1 min in UHV and cooled down to a given temperature. Hydrogen gas was introduced into the upstream chamber in stepwise by supplying H_2 gas of the same pressure as before to the backside of VLV. The H_2 pressure in the upstream chamber did not reach 1×10^{-5} Pa but $2\text{-}3 \times 10^{-6}$ Pa rapidly. This pressure difference is due to pumping by the membrane. The sticking coefficient α_m was estimated from this pressure difference. In this case, not only the membrane but Nb strip below the membrane should contribute to the H_2 absorption, and hence α_m was estimated from the total surface area of membrane and Nb strip.

In high temperature region where $T > 1273$ K, H_2 gas was introduced into the upstream chamber up to 4×10^{-4} Pa, and the membrane was heated up to a given temperature quickly. The pressure of H_2 dropped sharply owing to the atomization at the membrane surface and subsequent pumping of atoms by the chamber wall. The sticking coefficient α_m was estimated from the extent of pressure drop by assuming that α_m is equal to the atomization rate and all atoms produced are adsorbed on the chamber wall. The Nb strip

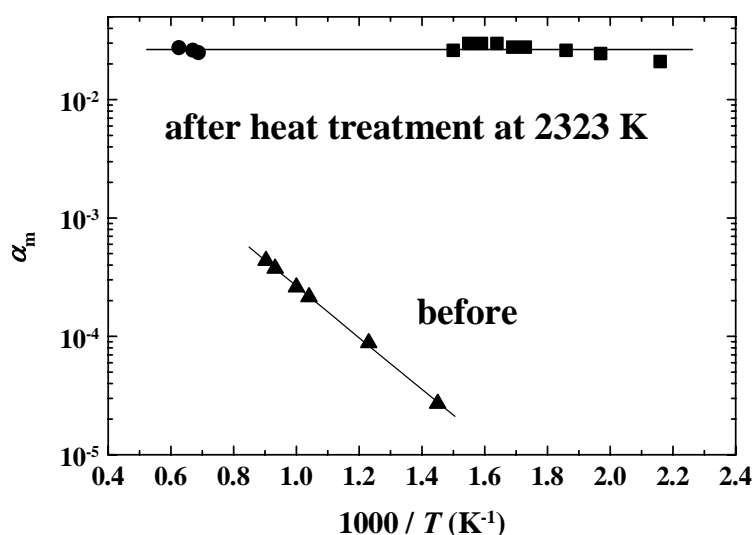


Fig. 8 Temperature dependence of α_m before and after heat treatment at 2323 K.

should contribute to this atomization, too. Hence surface area of the strip is considered in the estimation of α_m also in this case.

The sticking coefficient α_m thus obtained is plotted in Fig. 8 together with that measured before high temperature heat treatment in the previous section. It should be emphasized that α_m increased significantly by high temperature heating. In addition, the values of α_m determined by two different methods are on the same straight line parallel to the horizontal axis. Namely, no temperature dependence was observed in α_m after high temperature heating. This observation indicates that the potential barrier against dissociative chemisorption E_C is almost zero. Hence, the surface is considered to be clean. The values of α_m shown in Fig. 8, however, are still smaller than that of clean Nb surface (ca. 0.1). This discrepancy was ascribed to the overestimation of surface area contributing to the H_2 absorption and atomization. Such overestimation was caused by non-uniform temperature distribution during high temperature heating. The temperature of a part of Nb strip just beneath the membrane was slightly higher than other part of the strip and the membrane. Therefore, the surface of this part is considered to be cleaner than other part. It is plausible that this particular part played the dominant role in H_2 absorption and atomization. The new membrane is under construction at the present by taking account of this problem. It is, however, clear that the surface cleaned by high temperature heating was not contaminated by impurities during absorption and atomization experiments. Therefore, it can be safely concluded that the present apparatus has capability to carry out permeation and absorption/desorption experiments with clean surfaces.

4. Conclusions

A new apparatus was constructed to examine gas-, atom- and plasma-driven permeation of hydrogen isotopes through group VA metal membranes with precisely controlled surface states. Absorption/desorption experiments are also possible. This apparatus consists of two vacuum chambers, an upstream chamber and a downstream chambers, separated by a specimen membrane.

Both chambers are evacuated by turbo-molecular pumps and sputter-ion pumps. The upstream chamber is equipped with Ta filaments serving as atomizers in atom-driven permeation experiments and cathodes in plasma-driven permeation experiments. The specimen membrane is formed into a tubular shape and electrically isolated from the chamber. Hence, ohmic heating of the membrane is possible, and this feature of membrane is suitable for surface cleaning by high temperature heating and impurity doping for the control of surface chemical composition through surface segregation. Both chambers were evacuated to 1×10^{-7} Pa after baking. The main component of residual gas was H_2 , and the partial pressures of impurity gases other than H_2 were ca. 1×10^{-8} Pa. Gas- and atom-driven permeation experiments were successfully carried out with hydrogen gas for Nb membrane activated by heating in vacuum at 1173 K. Superpermeation was observed in the atom-driven permeation experiments. The absorption experiments with clean surface were also carried out. The surface was cleaned only in part, because the temperature distribution was not uniform during high temperature heating. Nevertheless, vacuum conditions were enough good to retain surface cleanliness during absorption experiments. Design of new membrane assembly was started to obtain uniform temperature distribution.

References

- [1] R. Hayakawa, A. Busnyuk, Y. Hatano, A. Livshits and K. Watanabe, *Physica Scripta*, in press.
- [2] A. I. Livshits, M. E. Notkin and A. A. Sammartsev, *J. Nucl. Mater.*, **170** (1990) 79.
- [3] F. Waelbroeck, Influence of Bulk and Surface Phenomena on the Hydrogen Permeation through Metals, Forschungszentrum Jülich report, Jül-1966, 1984.
- [4] H. Hackfort, K. Bösche, F. Waelbroeck, J. Winter and P. Wienhold, *J. Nucl. Mater.*, **144**(1987)10.
- [5] A. I. Livshits, M. E. Notkin, V. I. Pistunovich, M. Bacal and A. O. Busnyuk, *J. Nucl. Mater.*, **220-222**(1995)259.

- [6] A. I. Livshits, N. Ohyabu, M. Bacal, Y. Nakamura, A. Busnyuk, M. Notkin, V. Alimov, A. Samartsev, H. Suzuki and F. Sube, *J. Nucl. Mater.*, **266-269** (1999) 1267.
- [7] Y. Nakamura, S. Sengoku, Y. Nakahara, N. Suzuki, H. Suzuki, N. Ohyabu, A. Busnyuk, M. Notkin and A. Livshits, *J. Nucl. Mater.*, **278** (2000) 312.
- [8] Y. Nakamura, N. Ohyabu, H. Suzuki, Y. Nakahara, A. Livshits, M. Notkin, V. Alimov and A. Busnyuk, *Fusion Eng. Des.*, **49-50** (2000)899.
- [9] A. I. Livshits, Y. Hatano and K. Watanabe, *Fusion Sci. Technol.*, **41**(2002)882.
- [10] T. Tamura, T. Kuriwa, T. Amemiya, T. Fuda, A. Kamegawa, H. Takamura and M. Okada, *Mater. Trans., JIM*, **40**(1999)431.
- [11] T. Kuriwa, T. Tamura, T. Amemiya, A. Kamegawa, H. Takamura and M. Okada, *J. Alloys and Compounds*, **293-295**(1999)433.
- [12] C. Nishimura, M. Komaki and M. Amano, *Mater. Trans., JIM*, **32**(1991)501.
- [13] C. Nishimura, M. Komaki and M. Amano, *Trans. Mater. Res. Soc. Jpn.* **18B**(1994)1273.
- [14] C. Nishimura, M. Komaki, S. Hwang and M. Amano, *J. Alloys and Compounds*, **330-332**(2002)902.
- [15] M. A. Pick, J. W. Davenport, M. Strongin and G. Dienes, *Phys. Rev. Lett.*, **43**(1979)286.
- [16] M. A. Pick, *Phys. Rev. B*, **24** (1981)4287.
- [17] J. Völkl and G. Alefeld, *Hydrogen in Metals I*, Springer, Berlin, 1978, p.329.
- [18] K. Fujita, Y. C. Huang, and M. Tada, *Nippon Kinzoku Gakkaishi* **43** (1979)601.
- [19] M. A. Pick and K. Sonnenberg, *J. Nucl. Mater.* **131** (1985) 208.